Detecting critical supervision intervals during *in silico* chemotherapy treatments

Martin Ferenc Dömény[1], Melánia Puskás[1,2], Levente Kovács[1], Thi Thoa Mac[3], and Dániel András Drexler[1]

[1]Physiological Controls Research Center, University Research and Innovation Center, Óbuda University, Budapest, Hungary; domeny.martin@uni-obuda.hu, puskas.melania@uni-obuda.hu, kovacs@uni-obuda.hu, drexler.daniel@uni-obuda.hu
[2]Applied Informatics and Applied Mathematics Doctoral School, Óbuda University, Budapest, Hungary.
[3]Mechatronics Department, School of Mechanical Engineering, Hanoi University of Science and Technology, Hanoi, Vietnam; thoa.macthi@hust.edu.vn

Abstract: Nowadays, in many countries, the number of newly registered cancer patients keeps growing despite the recent advancements in the medical field. For this reason, every advancement that could potentially get humanity one step closer to fighting this disease is valuable. The future goal of our research is to create a device capable of measuring the tumor parameters of the patients and applying doses continuously. However, with the current technology, it is not possible since the measurement of the tumor states is not automatized. This study presents an intermediate step towards that goal by creating methods that can identify critical time intervals on which the treatments of patients should be supervised by investigating the tumor state in a hospital. To generate an optimal therapy, we used a genetic algorithm capable of generating a therapy for a group of patients with similar parameters. We used a mathematical model that contains the unique patient parameters to simulate the reaction of the tumor to the injected doses. According to the results, we can reduce the time spent in the hospital to almost a third of the original treatment time, based on in silico *tumor simulations.*

Keywords: genetic algorithm; therapy optimization; tumor model; drug scheduling

1 Introduction

Nowadays, medicine tries to treat cancer in several ways. There are local treatments, such as surgical procedures or radiation therapy, which can target a specific area of the body in a targeted method. The most commonly used treatment is chemotherapy, during which the patients receive a maximum dose tolerated by the patients at certain time intervals during the entire treatment. In addition to high toxicity, the large amounts usually also contribute to the development of drug resistance [1–3]. Today,

with the development of technology, a new direction has appeared. Computer simulations and optimization algorithms help to develop personalized treatments and implement them more cheaply, using less medicine [4].

Our research aims to increase the effectiveness of chemotherapy. During the research, we treated cancerous mice with chemotherapy drugs and estimated the parameters from the measurements obtained from them, which served as initial values for creating the best therapy [5, 6]. In the literature, several different approaches were used to develop chemotherapy, for example, fuzzy and model predictive systems [7, 8], neural networks [9–11], and global optimization methods, such as genetic algorithm [12, 13]. To optimize therapy, a mathematical model [14] is needed that can take into account the unique parameters of the patients [15, 16]. With the help of the model, we can simulate the reaction of the tumor to the administered doses [17].

The long-term goal of the research is a device similar to an artificial pancreas [18, 19], which can continuously monitor the parameters of the patient and the drug level in blood and the dynamics of the tumor and administer the drug accordingly. However, this is not yet possible with the current technology. Currently, the therapy is administered via injections, and with the help of different imaging modalities, we can gain insight into the processes taking place in the tumor [20]. Furthermore, we assume that the patient's tumor dynamics parameters are related to the other parameters of the patient, based on which we can cluster them into groups and apply optimal therapy created for that group.

The initial grouping can be done based on medical examinations and medical history. Then, a basic treatment is started for the patients in the same group. Since the parameters of the patients are not known to the doctor, it can turn out after the start of the treatment that some patients have been incorrectly grouped. One of our goals in this work is to determine the day the patient must go back for a control examination, and the volume of a tumor can be examined to see if the previous therapy has been effective. Based on our small animal experiments, it can be assumed that the parameters of the patients are not constant, i.e., they can change over time. Moreover, they change at the point when the volume of the tumor is greatly reduced (remission), after which it starts to grow again (relapse). So, our other goal is to detect this change since the change in the patient parameters may require a change in the used therapy. If the tumor begins to grow more aggressively, it may be necessary to use a therapy with higher doses for the given patient.

In this work, we also determined a day for the measurement to be carried out and a tumor volume threshold where regrouping should be done, with the help of which the given patient can be reassigned to another group after the changes in the parameters. With this procedure, it is possible to prevent the therapy from being ineffective or toxic for the patients and also reduce the time that the patients have to spend in the hospital.

Section 2 contains the mathematical model used to simulate tumor growth of the virtual patients acquired from real-world mice experiments and describes the previously created genetic algorithm that we used to generate an optimal therapy for a

group of similar patients. Section 3 describes the grouping problem we are solving in our research. In Section 4 we write about how the results were acquired using the real mice we had at our disposal and we detail the testing of the methods and summarize the results as well. Finally, in Section 5 we draw conclusions from the results and mention some ideas for future improvements.

2 Materials and methods

2.1 Mathematical model of tumor growth

A mathematical model is needed to simulate tumor growth and drug movement, which can be used to optimize therapy. Several mathematical models in the literature can describe tumor dynamics. Among the most frequently used models are the Gompertz and Hahnfeldt models. The Gompertz model [21, 22] is most often useful for the growth of animals and plants and the division of cancer cells. The other often used model, the Hahnfeldt model [23] uses non-linear equations for the dynamics of the tumor and vascular system, but without taking into account the movement of drugs within the body.

The mathematical model we use is a system of differential equations that includes linear expressions and some nonlinear terms. The equations describe pharmacokinetics, pharmacodynamics, and drug washout [24]. This system of differential equations can be written as [15, 16]:

$$\dot{x}_1 = (a-n)x_1 - b\frac{x_1 x_3}{ED_{50}+x_3}, \quad (1)$$

$$\dot{x}_2 = nx_1 + b\frac{x_1 x_3}{ED_{50}+x_3} - wx_2, \quad (2)$$

$$\dot{x}_3 = -(c+k_1)x_3 + k_2 x_4 + u, \quad (3)$$

$$\dot{x}_4 = k_1 x_3 - k_2 x_4. \quad (4)$$

The state variables in (1)-(4) represent different time functions. The time function of the living tumor volume is x_1 [mm^3], and the dead tumor volume is x_2 [mm^3]. The drug level of the central compartment is denoted by x_3 [mg/kg], which in our case is the time function of the level of the drug in the blood. The system input u, which is the injection rate [mg/kg/day], is injected into the central compartment. The time function of the level of the drug in the tissues is x_4 [mg/kg]. The parameters of the model are summarized in Table 1.

The model (1)-(4) assumes that the input u is continuous in time. During the experiments, the inputs are the injections. An injection can be modeled as an impulsive input. Let a dose u_i be assigned to each time point t_i, where $i = 1,2,\ldots,U$, where U is the number of injected doses. The input is therefore impulsive since the change in drug level due to the injection takes place in a very short time compared to the time constant of the system. We assume that the injections cause discontinuous changes

Parameter	Name	Dimension
a	proliferation rate coefficient	day^{-1}
b	drug efficiency rate coefficient	day^{-1}
n	necrosis rate coefficient	day^{-1}
w	washout rate coefficient of dead tumor cells	day^{-1}
ED50	median effective dose of the drug	$\text{mg} \cdot \text{kg}^{-1}$
c	clearance of the drug	day^{-1}
k1	flow rate coefficient of the drug from the central to peripheral compartment	day^{-1}
k2	flow rate coefficient of the drug from the peripheral to central compartment	day^{-1}

Table 1
The name and dimension of the model parameters.

in the drug level of the blood [15]:

$$x_3(t_i^+) = x_3(t_i^-) + u_i. \tag{5}$$

The output of the system is the total tumor volume (denoted by y), which is the sum of the living tumor volume and the dead tumor volume:

$$y = x_1 + x_2. \tag{6}$$

During the *in vivo* experiments, y is the measured variable since we can approximate the total tumor volume of the mice based on measurements made with a digital caliper. The measurement is extremely difficult, as the tumor is mostly amorphous and located under the skin. Since we can only measure the width and length of the tumor with the caliper, we approximate the total volume with a formula [25], and the noise in the measurements measured with a digital caliper is estimated using a noise model [26].

2.2 Therapy generation using genetic algorithm

In our previous work, we created a genetic algorithm capable of generating therapies for similar patients [12]. Then we examined the effects of different fitness and mutation functions to find the most effective therapy generation methods [13]. This study uses this genetic algorithm to generate an initial therapy. Then, we use this therapy to examine the patient groups and to see how different patients react to it. When we optimize chemotherapy, we have two obvious objectives in mind. We need to reduce the tumor volume of the patient, as well as the injected doses to reduce toxicity. The used fitness function can be written as follows [13]:

$$F_1 = \sum_{j=1}^{L} \left(\kappa + W_1 \sum_{i=1}^{N} U_i + W_2 Y_{end} \right), \tag{7}$$

where κ is given by

$$\kappa = R_1 \sum_{i=1}^{N} \left(\frac{\varphi_i}{Y_{max}} \right)^2 + R_2 \sum_{i=1}^{N} \left(\frac{U_i}{U_{max}} \right)^2, \tag{8}$$

and

$$\varphi_i = \begin{cases} Y_i - Y_{ref}, & \text{if } Y_i \geq Y_{ref}, \\ 0, & \text{otherwise.} \end{cases} \tag{9}$$

In these equations, R_1, R_2, W_1 and W_2 are weights. The summation in κ goes till $N = 105$, the number of genes in each individual. U_i is the injected dose on the day i. Y_i is the tumor volume of the patient on the i-th day, $Y_{ref} = 4$ is the reference tumor volume. L is the number of patients in our patient group and j denotes the current patient. The used selection function is the frequently used tournament selection [13, 27], and the crossover function is the Laplace crossover [13, 28]. The used mutation function implements an adaptive mutation, taking into account the fitness values of the individuals and applying mutation based on them [13].

This fitness function ensures that the tumor volume of the patients is close to the given reference volume and also minimizes the injected doses each day. In the function, we used the weighted sum approach, which is frequently used in multi-objective optimization, to reduce the complexity of the problem [29]. Two terminating constraints are also added to the function, to ensure that the patient is cured at the end of the treatment, and to further minimize cumulative dose.

3 Creating a set of patients

To create a therapy that is generally good for the set of patients, we need to make sure those patients have similar parameters. Otherwise, they will react to the treatment differently. If we can identify different clusters of patients, we can optimize therapy for the whole group. We assume when a patient visits the doctor, the doctor (based on the age, medical history, and physiological details of the patient) can assign the patient to a specific group, giving them the optimal treatment. After this initial classification, there are two problematic outcomes, as shown in Figure 1.

Either the patient was initially put into the wrong group by the doctor, or the parameters of the patient changed during the treatment. Both cases have to be detected and corrected. We devised a method for identifying critical days when the patients should be continuously monitored to correct these possible mistakes. This method gives a reference for the doctor on when to check patients to modify treatment. In Figure 1, T_1, T_2 and T_3 are the treatment groups, each patient gets the same treatment in the same group. The black crosses are the patients, which are described by their set of parameters (a, b, n, w, ED_{50}, c, k_1 and k_2).

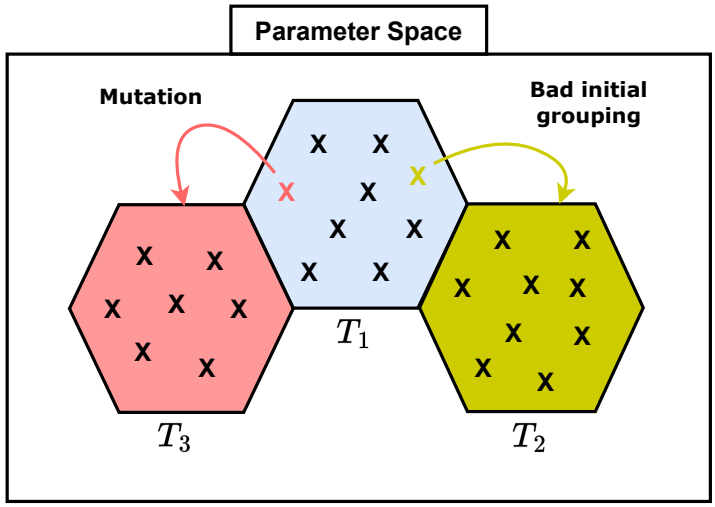

Figure 1
The representation of the grouping problem. First, the doctor groups the patient based on the patient's physiology into T_1. In case a mutation appears, the patient parameters will be in T_3. If the patient was not assigned to the correct group, the patient's parameters are in group T_2 (which may overlap with T_3, but it is distinct in the figure for the sake of simplicity).

4 Results

4.1 Grouping patients based on their parameters

To determine the critical intervals, we generated 10,000 random virtual patients. Initially, we had 54 parameters taken from *in vivo* mouse experiments, but this amount is insufficient to develop any reliable method. We assume that the distribution of mice parameters can be expressed as a normal distribution. We generated 10,000 random mice parameter sets with random numbers taken from a normal distribution, with the deviation and the expected value taken from the original dataset.As the next step, we calculated the ratios of the normalized a and b parameters of each virtual patient. Parameter a is the tumor proliferation rate, and b is the maximal drug effect. These two parameters are the most sensitive in the model (1)-(4), so their value affects the output of the system (tumor volume) the most [30].

In Figure 2, we can see the parameter ratios of the virtual patients, marked with blue dots. At the bottom of the figure are the patients with lower a parameters combined with higher b parameters. These patients react better to a given treatment and are more likely to be cured with lower doses. Moving upwards in the figure, there are the patients with higher a parameters with lower b parameters. These patients are harder to cure as they have more aggressive tumors that are more resistant to the drugs.

We marked the mean of the ratios with a red dashed line and a constant k times the standard deviation of the ratios with a black dashed line. We used this black line

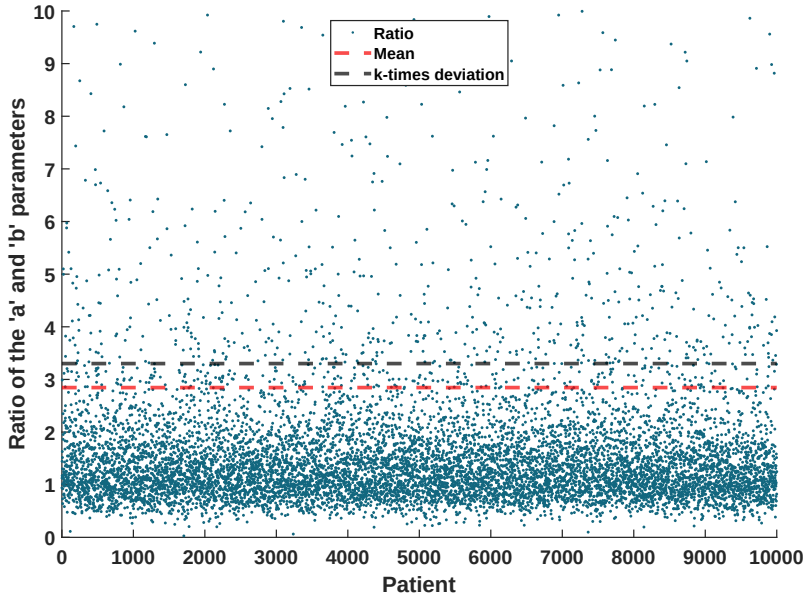

Figure 2
Scatter plot representing the ratio of the a and b parameters of the virtual patients. The red line represents the mean of the ratios, and the black line is k times the standard deviation of the ratios. We separate the patients based on the black line, with different k values. In the figure, $k = 0.075$.

to create two groups of patients called group A and group B (group A formed from the patients below the line). We then generated one treatment for group A using the genetic algorithm detailed in Subsection 2.2. After we generated the optimal treatment for group A, we applied this treatment to group A and B at the same time and simulated the reaction of the tumors to the therapy. As the next step, we took the highest tumor volume in group A each day and plotted it along with the lowest tumor volume each day from group B. This can be seen in Figure 3.

This gave us two points when the two curves intersect, and they will be used to point out the critical intervals. The first intersection indicates the first scenario, where the patients were initially placed in the wrong group, and the second intersection indicates that a parameter change has occurred, suggesting the need for an adjustment in the treatment protocol. We repeated this process 200 times with different k values ranging from -0.1 to 0.1, giving us a range around the mean of the ratios. Using k values outside this range rarely gave us intersections, as the two groups (A and B) were mixed. After we got these points for different k values, we calculated the mean and deviation of the time and tumor volume at these intersections. In Figure 4, we randomly selected 100–100 patients from groups A and B and simulated their tumor volume with the generated treatment. We also marked the mean of the days we got at these intersections with a vertical black dashed line and the distance equal to the standard deviation in both positive and negative directions with vertical red dashed lines. With horizontal dashed lines, we marked the same mean and deviation but of

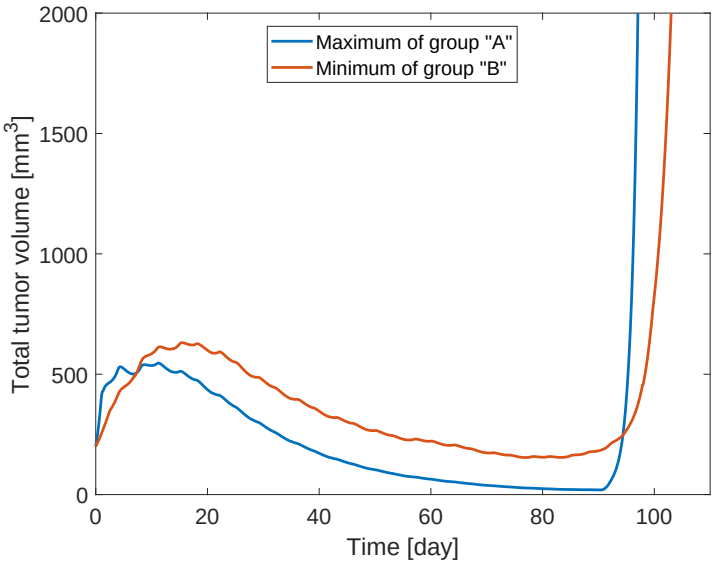

Figure 3
The intersections given by the best and the worst tumor simulation from both groups. The blue line represents the highest tumor volume each day from group *A*, and the red line represents the lowest tumor volume from group *B* each day.

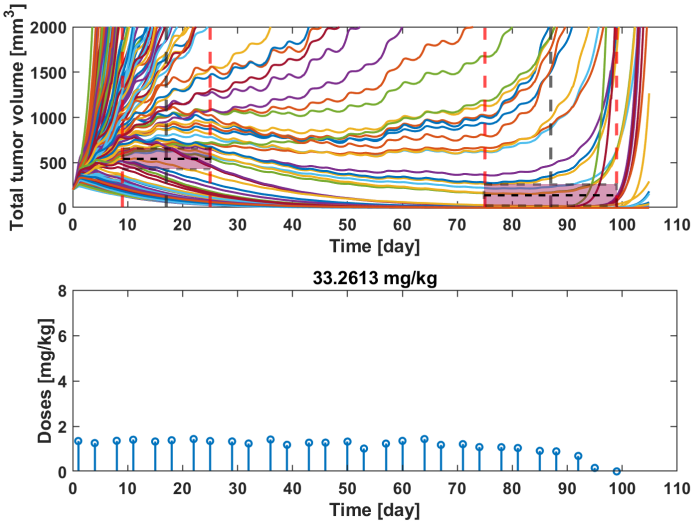

Figure 4
The intervals given by the mean and deviation of the intersections. The top of the figure contains the tumor volume simulations of 200 randomly selected patients from groups *A* and *B* with respect to time. The bottom of the plot represents the injected doses. On the top, the black dashed line marks the mean of the critical days. The red dashed lines mark the distance of deviation from the mean in positive and negative directions. These lines mark the critical intervals on when the patients should be checked.

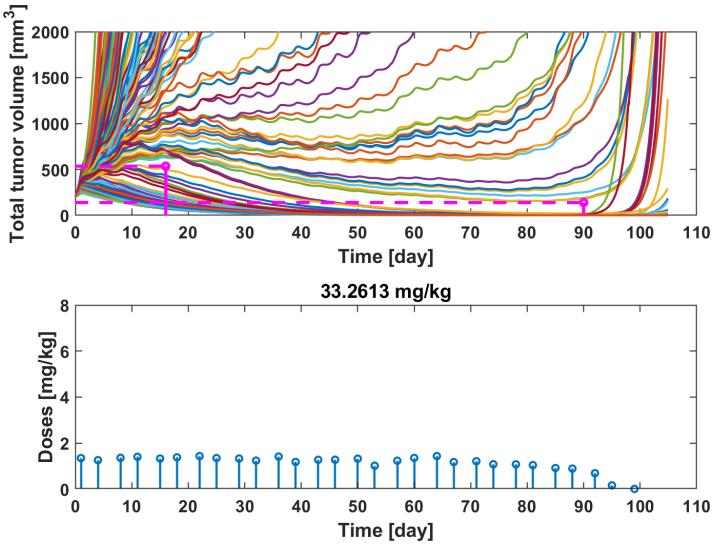

Figure 5
The intervals given by the median of the intersections. The top of the figure contains the tumor volume simulations of 200 randomly selected patients from groups *A* and *B* with respect to time. The bottom of the plot represents the injected doses. The magenta spikes are the median of the tumor volumes and the days given by the two intersections.

the tumor volumes at the intersections. These lines gave us two magenta rectangles at the beginning and the end of the treatments. The first rectangle gives a critical interval when it turns out that the patients were misclassified initially, and the second rectangle shows when we should check for parameter changes.

4.2 Testing critical intervals on *in silico* patients

During our research, we had 54 mice parameters at our disposal. To test the intervals we got in Subsection 4.1, we used these mice parameters as patients. We first simulated the tumor volumes of these patients using the therapy generated in the previous section. In Figure 6, we marked the intervals given by the mean and the deviation of the intersection from Subsection 4.1. The first interval indicates the scenario of bad initial grouping, while the second indicates the scenario of parameter changes. Using the indicated lines, we can define two methods. The first method examines the intersections of the mean lines of the critical time and tumor volumes (indicated with black dashed lines in Figure 6). Using this method, the patients only have to spend two days in the hospital. The patient should be reassigned to a different group if their tumor volume is above the threshold (indicated with the horizontal black dashed line). Otherwise, the current treatment is sufficient.

Using this method, we can correctly find two patients at the first intersection, but we would also incorrectly migrate two other patients to different groups because they are above the threshold even though they have decreasing tumor volumes. In

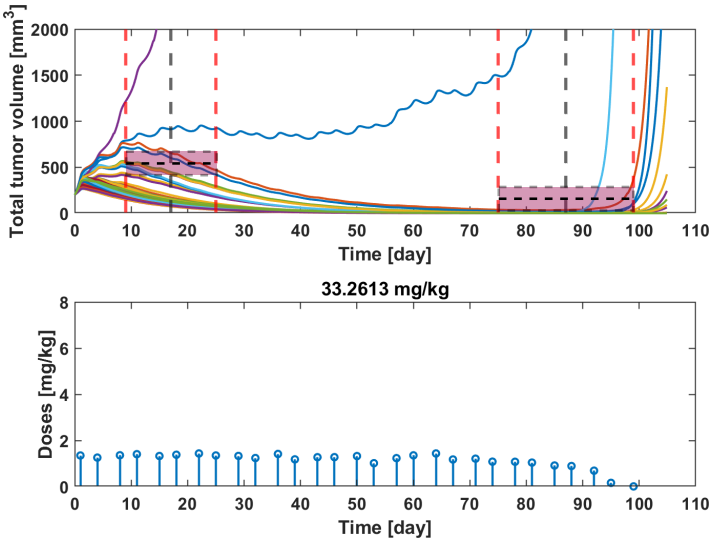

Figure 6
The intervals given by the mean and deviation of the intersections, were applied on the 54 test patients taken from mouse experiments. The top figure contains the total tumor volumes of patients with respect to time. The bottom figure contains the injected doses. The first interval represents the bad initial grouping scenario, while the second one indicates parameter changes.

addition, the second intersection would filter zero patients because the parameter changes only occur after the intersection. The advantage of this method, however, is that the patients only have to be measured two times during the 105-day treatment (given that they can administer the doses outside the hospital). The second method uses intervals given by the mean of the intersections and the deviation of the intersections, marked with magenta rectangles in Figure 6. This gives us wider intervals, so more opportunities to correct the treatments, but the patients have to spend more time in the hospital. Looking at the second interval from day 76 to 98, we can detect parameter changes for some patients, however, we still could not identify all of them, since many patients start experiencing relapse after the 100th day. For the first interval, from day 9 to day 26, we could measure the patients many times so we could detect if their tumor shows a decreasing tendency and prevent incorrect treatment modifications.

In Figure 7 we can see the median of the intersections from Subsection 4.1, marked with magenta spikes. Similarly to the last figure, we can define two methods here. First, by checking only these points, we can get similar results. The first point would filter out four patients, two of which are incorrect. The second point would still not filter anyone because the relapse happens after the day of examination. The other method, however, could provide better results. If we use these marked median points as boundaries of intervals, we can detect almost all the patients that do not fit in the groups. The first interval should go from day zero to day 16, between the two points the patients do not need to be measured, and the second interval should start

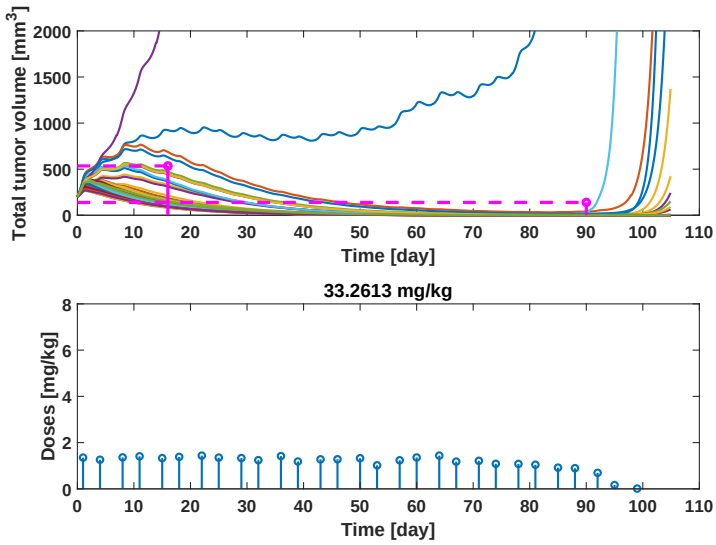

Figure 7
The points given by the median of the intersections, marked on the tumor volume simulations of 54 test patients taken from mouse experiments. The top figure contains the total tumor volumes of patients with respect to time. The bottom figure contains the injected doses.

at day 90 until the end of the treatment. Using this method, we can detect all the incorrectly grouped patients in the first interval (even detect the decreasing tumor volumes to prevent incorrect grouping). Also, with this method, we can detect all relapses due to parameter changes after day 90. A possible explanation for why the median method provided the best results is that during the experiments, many outlier values were present that potentially skewed the mean using methods. The median is a more robust way to describe data and is not sensitive to outliers.

Table 2 contains the summary of the results of the test patients. As shown in the table, using only the intersections as separation points, the patients have to spend the least amount of time with examinations. Still, there is little chance of identifying bad grouping, both in the case of mean and median methods. Examining the interval

Method	Correct reassignment [number of patients]	Time spent in the hospital [day]
Mean of the intersections	2 / 16	2
Interval given by mean and deviation	7 / 16	40
The median of the intersections	2 / 16	2
Intervals given by the median	16 / 16	31

Table 2
Summary of the four methods. In the second column, the first number indicates the correct reassignments and the second number indicates the number of patients that should be reassigned.

given by the mean plus the deviations provides better results, but the patients have to spend significantly more time in the hospital. Using the fourth method, we could detect all the bad groupings, with only 31 days spent in the hospital.

5 Conclusion

In this study, we devised methods for finding and correcting bad patient grouping during chemotherapy treatment. The treatment was generated using a previously created genetic algorithm [12, 13]. These methods can give a reference to the doctors on when to check patients to adjust the treatment they receive. They could be used in the future when the technology allows the patients to self-administer the drug. According to the results, the four different methods provided varying results, however using the medians of the intersection (discussed in Subsection 4.1.) we could identify two critical intervals, where the possible treatment adjustments can be made. Outside these intervals, the patients could leave the hospital (given they can self-administer the drugs). Shortening the time spent in the hospital could have positive benefits to the mental health of the patients, increasing the chances of recovery. Of course, these methods have limitations, which need to be solved in the future before they can be applied in practice. We assumed the patient parameters change with a fixed amount when they approach zero tumor volume, which could differ in reality. Additionally, tumor volume may not entirely correlate with the severity of the disease, so other indicators are needed to increase accuracy. The used tumor model can also be improved since it does not take into account the toxic effect of the drug on healthy cells. In the future, the method to find the critical intervals could be improved using machine learning techniques or other optimization and clustering methods. Improving the genetic algorithm could also improve the therapy generation. Integrating multi-objective optimization algorithms into the therapy generation could create a more efficient treatment generation method [31–33].

Acknowledgment

Project no. 2019-1.3.1-KK-2019-00007. has been implemented with the support provided from the National Research, Development and Innovation Fund of Hungary, financed under the 2019-1.3.1-KK funding scheme. This project has been supported by the Hungarian National Research, Development and Innovation Fund of Hungary, financed under the TKP2021-NKTA-36 funding scheme. The work of Dániel András Drexler was supported by the Starting Excellence Researcher Program of Óbuda University, Budapest Hungary. Melánia Puskás is also with the Óbuda University, Applied Informatics and Applied Mathematics Doctoral School, Budapest, Hungary. Melánia Puskás was supported by the ÚNKP-23-3 New National Excellence Program of the Ministry for Culture and Innovation from the source of the National Research, Development and Innovation Fund. Martin Ferenc Dömény was supported by the ÚNKP-23-2 New National Excellence Program of the Ministry for Culture and Innovation from the source of the National Research, Development and Innovation Fund. On behalf of the ”Kemoterápiás kezelések *in silico* optimalizálása” project we are grateful for the possibility to use HUN-REN

Cloud (see Héder et al. 2022; https://science-cloud.hu/) which helped us achieve the results published in this paper [34].

References

[1] I. Kareva, D. J. Waxman, and G. Lakka Klement. Metronomic chemotherapy: An attractive alternative to maximum tolerated dose therapy that can activate anti-tumor immunity and minimize therapeutic resistance. *Cancer Letters*, 358(2):100–106, 2015.

[2] N. André, S. Banavali, Y. Snihur, and E. Pasquier. Has the time come for metronomics in low-income and middle-income countries? *The Lancet Oncology*, 14(6):e239–e248, 2013.

[3] A. Romiti, M. C. Cox, I. Sarcina, R. D. Rocco, C. D'Antonio, V. Barucca, and P. Marchetti. Metronomic chemotherapy for cancer treatment: a decade of clinical studies. *Cancer Chemotherapy and Pharmacology*, 72(1):13–33, 2013.

[4] C. de Martel, D. Georges, F. Bray, J. Ferlay, and G. M. Clifford. Global burden of cancer attributable to infections in 2018: a worldwide incidence analysis. *Lancet Glob Health*, 8(2):e180–e190, 2019.

[5] L. Kovács, T. Ferenci, B. Gombos, A. Füredi, I. Rudas, G. Szakács, and D. A. Drexler. Positive impulsive control of tumor therapy—a cyber-medical approach. *IEEE Transactions on Systems, Man, and Cybernetics: Systems*, pages 1–12, 2023.

[6] B. Gergics, F. Vajda, A. Ládi, A. Füredi, and D. A. Drexler. Pharmacodynamics modeling based on in vitro 3d cell culture experiments. In *2023 IEEE 17th International Symposium on Applied Computational Intelligence and Informatics (SACI)*. IEEE, May 2023.

[7] T. D. Szűcs, M. Puskás, D. A. Drexler, and L. Kovács. Model predictive fuzzy control in chemotherapy optimization. In *2023 IEEE 17th International Symposium on Applied Computational Intelligence and Informatics (SACI)*, pages 103–108, 2023.

[8] T. D. Szűcs, M. Puskás, D. A. Drexler, and L. Kovács. Model predictive fuzzy control in chemotherapy with hessian based optimization. In *2024 IEEE 22nd World Symposium on Applied Machine Intelligence and Informatics (SAMI)*, pages 211–216, 2024.

[9] L. Kisbenedek, M. Puskás, L. Kovács, and D. A. Drexler. Indirect supervised fine-tuning of a tumor model parameter estimator neural network. In *2023 IEEE 17th International Symposium on Applied Computational Intelligence and Informatics (SACI)*, pages 000109–000116, 2023.

[10] L. Kisbenedek, M. Puskás, L. Kovács, and D. A. Drexler. Clustering-based parameter estimation of a tumor model. In *2023 IEEE 21st Jubilee International Symposium on Intelligent Systems and Informatics (SISY)*, pages 43–48, 2023.

[11] M. Puskás and D. A. Drexler. Tumor model parameter estimation for therapy optimization using artificial neural networks. In *2021 IEEE International Conference on Systems, Man, and Cybernetics (SMC)*, pages 1254–1259, 2021.

[12] M. F. Dömény, M. Puskás, L. Kovács, and D. A. Drexler. In silico chemotherapy optimization with genetic algorithm. In *2023 IEEE 17th International Symposium on Applied Computational Intelligence and Informatics (SACI)*, pages 97–102. IEEE, May 2023.

[13] M. F. Dömény, M. Puskás, L. Kovács, and D. A. Drexler. Population-based chemotherapy optimization using genetic algorithm. In *2023 IEEE 21st International Symposium on Intelligent Systems and Informatics (SISY)*, pages 23–28. IEEE, September 2023.

[14] B. Gergics and D. A. Drexler. Mathematical modeling of tumor based on in vitro and in vivo data, and in vitro to in vivo extrapolation and its challenges: a literature review. In *2023 IEEE 23rd International Symposium on Computational Intelligence and Informatics (CINTI)*, pages 291–298, 2023.

[15] D. A. Drexler, T. Ferenci, A. Füredi, G. Szakács, and L. Kovács. Experimental data-driven tumor modeling for chemotherapy. In *Proceedings of the 21st IFAC World Congress*, pages 16466–16471, 2020.

[16] D. A. Drexler, T. Ferenci, A. Lovrics, and L. Kovács. Tumor Dynamics Modeling based on Formal Reaction Kinetics. *Acta Polytechnica Hungarica*, 16:31–44, 2019.

[17] F. Kulcsár, D. Békevári, G. Eigner, D. A. Drexler, A. V. Patai, T. Micsik, and R. Fleiner. Development of machine learning based colorectal cancer subtype classificator. In *2021 IEEE 21st International Symposium on Computational Intelligence and Informatics (CINTI)*, pages 000049–000053, 2021.

[18] S. J. Moon, I. Jung, and C.-Y. Park. Current advances of artificial pancreas systems: A comprehensive review of the clinical evidence. *Diabetes &amp Metabolism Journal*, 45(6):813–839, 2021.

[19] P. Szalay, D. A. Drexler, and L. Kovács. Exploring robustness in blood glucose control with unannounced meal intake for type-1 diabetes patient. *Acta Polytechnica Hungarica*, 20:27–46, 2023.

[20] G. Katti, S. A. Ara, and A. Shireen. Magnetic resonance imaging (mri)–a review. *International journal of dental clinics*, 3(1):65–70, 2011.

[21] M. C. Tjørve, Kathleen and E. Tjørve. The use of Gompertz models in growth analyses, and new Gompertz-model approach: An addition to the unified-richards family. *PLOS ONE*, 12(6):1–17, 2017.

[22] C. Vaghi, A. Rodallec, R. Fanciullino, J. Ciccolini, J. P. Mochel, M. Mastri, C. Poignard, J. M. L. Ebos, and S. Benzekry. Population modeling of tumor growth curves and the reduced gompertz model improve prediction of the age of experimental tumors. *PLOS Computational Biology*, 16(2):1–24, 2020.

[23] P. Hahnfeldt, D. Panigrahy, J. Folkman, and L. Hlatky. Tumor development under angiogenic signaling: A dynamical theory of tumor growth, treatment response, and postvascular dormancy. *Cancer Research*, 59:4770–4775, 1999.

[24] B. Meibohm and H. Derendorf. Basic concepts of pharmacokinetic/pharmacodynamic (pk/pd) modelling. *International Journal Of Clinical Pharmacology And Therapeutics*, 35:401–413, 1997.

[25] J. Sápi, L. Kovács, D. A. Drexler, P. Kocsis, D. Gajári, and Z. Sápi. Tumor volume estimation and quasi-continuous administration for most effective bevacizumab therapy. *PLOS ONE*, 10(11):e0142190, 2015.

[26] M. Puskás, B. Gergics, B. Gombos, A. Füredi, G. Szakács, L. Kovács, and D. A. Drexler. Noise modeling of tumor size measurements from animal experiments for virtual patient generation. In *2023 IEEE 27th International Conference on Intelligent Engineering Systems (INES)*. IEEE, 2023.

[27] B. L. Miller and D. E. Goldberg. Genetic algorithms, tournament selection, and the effects of noise. *Complex Syst.*, 9, 1995.

[28] K. Deep, K. Singh, M. Kansal, and C. Mohan. A real coded genetic algorithm for solving integer and mixed integer optimization problems. *Applied Mathematics and Computation*, 212:505–518, 06 2009.

[29] J. Shi, O. Alagoz, F. S. Erenay, and Q. Su. A survey of optimization models on cancer chemotherapy treatment planning. *Annals of Operations Research*, 221(1):331–356, March 2011.

[30] M. Siket, G. Eigner, and L. Kovács. Sensitivity and identifiability analysis of a third-order tumor growth model. In *2020 IEEE 15th International Conference of System of Systems Engineering (SoSE)*, pages 417–422, 2020.

[31] M. Siket, I. Jánoki, A. Nagy, and P. Földesy. Sample-in-the-loop laser speckle contrast imaging based on optimization. *Acta Polytechnica Hungarica*, 20:25–39, 2023.

[32] A. Petrovski, J. McCall, and B. Sudha. Multi-objective optimization of cancer chemotherapy using swarm intelligence. In *AISB 2009 Symposium on Adaptive and Emergent Behaviour and Complex Systems*. Citeseer, 2009.

[33] T. T. Mac, C. Copot, D. T. Tran, and R. D. Keyser. A hierarchical global path planning approach for mobile robots based on multi-objective particle swarm optimization. *Applied Soft Computing*, 59:68–76, 2017.

[34] M. Héder, E. Rigó, D. Medgyesi, R. Lovas, S. Tenczer, F. Török, A. Farkas, M. Emődi, J. Kadlecsik, G. Mező, Á. Pintér, and P. Kacsuk. The past, present and future of the ELKH cloud. *Információs Társadalom*, 22(2):128, aug 2022.